The Journal of Supercritical Fluids 140 (2018) 364–371

Contents lists available at ScienceDirect

The Journal of Supercritical Fluids

journal homepage: www.elsevier.com/locate/supflu

Production of copaiba (*Copaifera officinalis*) oleoresin particles by supercritical fluid extraction of emulsions

José Luis Pasquel Reátegui[a], Flavia P. Fernandes[a], Philipe dos Santos[a], Camila A. Rezende[b], Adilson Sartoratto[c], Carmen Lucia Queiroga[c], Julian Martínez[a,*]

[a] School of Food Engineering, Food Engineering Department, University of Campinas, 13083-862 Campinas, SP, Brazil
[b] Institute of Chemistry, University of Campinas, 13083-862 Campinas, SP, Brazil
[c] Chemical, Biological and Agricultural Pluridisciplinary Research Center (CPQBA), University of Campinas, 13083-970 Campinas, SP, Brazil

GRAPHICAL ABSTRACT

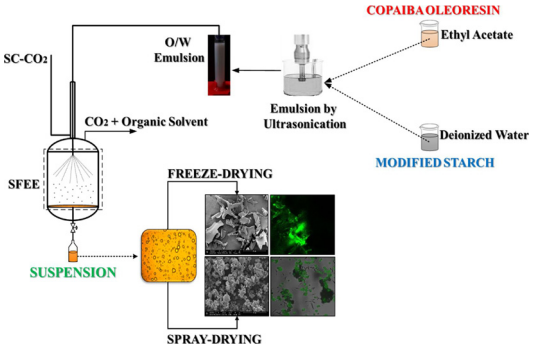

ARTICLE INFO

Keywords:
Copaiba
Nanosuspension
SFEE
β-Caryophyllene
X-ray diffraction
Confocal
Microscopy

ABSTRACT

Suspended particles of copaiba (*Copaifera officinalis*) oleoresin were produced by supercritical fluid extraction of emulsions (SFEE), using modified starch Hi-Cap 100® as core material. First, ultrasound was applied to produce oil in water (O/W) emulsions with droplet diameter of 261.7 ± 2.2 nm. In SFEE, CO_2 and emulsion flow rates, and solvent extraction time were evaluated in terms of residual ethyl acetate content (REA) and β-caryophyllene recovery in the suspension. SFEE achieved 94.1% reduction of ethyl acetate and β-caryophyllene recovery of 7.3%. This REA is within the exposure limit of ethyl acetate (5000 ppm per day). The suspended nanoparticles' size showed little variation from the emulsion droplet diameter. Finally, the suspensions were dried to obtain powder particles. Field emission scanning electron microscopy (FESEM) revealed different structures depending on the drying method (freeze-drying or spray-drying). Moreover, confocal laser scanning microscopy (CLSM) confirmed that copaiba oleoresin was encapsulated in the particles.

1. Introduction

Copaiba (*Copaifera officinalis*) is a tree, native to South America, which produces an oleoresin with medicinal properties, such as anti-inflammatory [1], anticancer [2], antitetanic and antiseptic, besides being indicated to treat syphilis, bronchitis, and wounds [3]. Copaiba oleoresin is mainly composed by hydrocarbon sesquiterpenes (about 90%), among them, β-caryophyllene is the major component and

* Corresponding author.
E-mail address: julian@unicamp.br (J. Martínez).

https://doi.org/10.1016/j.supflu.2018.07.021
Received 11 April 2018; Received in revised form 19 July 2018; Accepted 20 July 2018
Available online 23 July 2018

considered responsible for its biological activity [4,5]. However, copaiba oleoresin cannot be directly ingested, because of its unpleasant taste [6]. Moreover, it has low solubility in water but is soluble in some organic solvents.

Encapsulation of active compounds has attracted the attention of researchers in this field, and techniques using supercritical fluids, mainly carbon dioxide (CO_2), have been developed to face the disadvantages of conventional techniques like nanoprecipitation, spray-drying, freeze-drying and solvent evaporation of emulsions. According to Santos et al. [7] one of the most widespread and simple encapsulation techniques is the evaporation of the solvent from an oil-in-water emulsion (O/W). Organic solvents can generally be removed by evaporation, allowing the production of micro or nanometric particles [8]. However, the production of gas bubbles during solvent evaporation can modify the structure of the emulsion, resulting in low encapsulation efficiency [9]. Supercritical fluid technologies can contribute to eliminating this problem since it avoids the exposure of the product to high temperatures for extended times. Besides, because of the high solubility of organic solvents in supercritical CO_2, this technology is appropriate to reduce the concentration of residual organic solvents in the final suspension.

Supercritical fluid extraction of emulsions (SFEE) is based on the extraction of the organic solvent from emulsion droplet using supercritical CO_2 (SC-CO_2), which has advantages such as moderate critical point, non-toxicity and environmental safety [10]. SFEE combines emulsion techniques and the supercritical antisolvent (SAS) precipitation process (SAS). According to Della Porta et al. [11], with this combination, the particles size can be controlled from the initial emulsion droplet size. Several works have applied SFEE to natural compounds and polymers, obtaining a correspondence between the droplet and the particle size distributions [12]. This technique can also reduce the time for solvent removal and polymer precipitation [13]. SFEE has been successfully applied in the formation of β-carotene suspended particles from an O/W emulsion using dichloromethane as a solvent [14], particles containing capsaicinoids from red pepper [15], encapsulated carotenoids (lycopene and β-carotene) in modified starch to be used as antioxidants and dyes [7] and other compounds with pharmaceutical applications [16–18].

In this work SFEE was applied for the encapsulation of copaiba oleoresin, focusing on β-caryophyllene as the target compound. The influence of CO_2 flow rate, emulsion flow rate and organic solvent extraction time were evaluated in terms of residual ethyl acetate content, concentration of β-caryophyllene in the particles, mean particle diameter and oleoresin loss. The suspension obtained after SFF were dried by *freeze-drying and spray-drying* and then characterized for their moisture content, water activity, particle size distribution, X-ray diffraction and particle morphology by field emission scanning electron microscopy (FESEM) and confocal laser scanning microscopy (CLSM).

2. Materials and methods

2.1. Material

Modified starch Hi-Cap 100® donated by Ingredion Brazil Industrial Ingredients Ltda. (Mogi Guaçu-SP, Brazil) was used as the core material. Ethyl acetate 99.5% (Dinâmica, São Paulo, Brazil) was used as organic solvent in the emulsions. Carbon dioxide (CO_2) with 99.9% purity (White Martins, Campinas, Brazil) was used as supercritical antisolvent in SFEE. The standard used in gas chromatography coupled to mass spectrometry (GC–MS) was (−)-*trans*-caryophyllene (98.5% purity), which was purchased from Sigma-Aldrich (Sao Paulo, Brazil).

Copaiba (*Copaifera officinalis*) oleoresin was purchased from Ferquima Indústria Comercio LTDA (Vargem Grande Paulista, Brazil) and stored at 5 °C until emulsion preparation.

2.2. Preparation of the emulsion

The emulsification condition that provided droplets with the smallest size and the greatest kinetic stability for the encapsulation of copaiba oleoresin by SFEE were selected from a previous work [19]. Briefly, 200 mL of emulsion were prepared for each SFEE experiment with the following procedure: 1.2 g of copaiba oleoresin was dissolved in 30 mL of ethyl acetate, and 3.4 g of modified starch (Hi-Cap 100®) was separately dissolved in 170 mL of deionized water. The modified starch solution was let to rest for two hours at room temperature to ensure its complete saturation. The oleoresin and starch solutions were mixed with a magnetic stirrer for 3 min to obtain a homogeneous dispersion. Finally, the dispersion was emulsified at 480 W for 6 min with an ultrasound probe (Unique, Model DES500, Campinas-SP, Brazil). The variation of the droplet mean diameter with time after emulsification was investigated to establish the appropriate moment to inject the emulsion in the SFEE unit.

2.3. Supercritical fluid extraction of emulsion

The extraction of the organic solvent from the emulsion was carried out in a homemade SFEE unit (Fig. 1), which contains a CO_2 supply system, an emulsion injection system and a high-pressure stainless-steel column. The supercritical solvent used in SFEE must have high affinity to the organic solvent and low affinity to the target compound to achieve proper extraction. Briefly, CO_2 was initially cooled in a thermostatic bath (MA184, Marconi, Campinas, Brazil) to –5 °C, then pressurized using a pneumatic pump (PP 111-VE MBR, Maximator, Nordhausen, Germany) and subsequently heated to the operating temperature in a heating bath (MA184, Marconi, Campinas, Brazil). Then, supercritical CO_2 was injected into the high-pressure column (712 ml of internal volume) at a flow rate controlled by a micrometer valve. After stabilization of temperature and pressure, the emulsion was injected into the high-pressure column through two different coaxial nozzles with an internal diameter of 177.8 and 122 µm, using a HPLC pump (PU-2080, Jasco, Tokyo, Japan). After the injection of the emulsion, the system was maintained under the operating conditions to remove the organic solvent (extraction time). Then, the column was slowly depressurized, keeping the CO_2 flow rate constant, and the suspension was collected and stored in amber glasses at −18 °C until the analyses.

To maximize the extraction of ethyl acetate, three CO_2 flow rates (Q_{CO2}, 12.48, 18.60 and 24.42 g/min) and two emulsion flow rates (Q_{em}, 0.5 and 1.0 mL/min) were tested. According to Della Porta and Reverchon [12], the mixture of ethyl acetate and CO_2 has the critical pressure of 8.5 MPa at 38 °C, and 0.9 M fraction of CO_2. Under these operating conditions, water is only slightly soluble in supercritical CO_2, whereas ethyl acetate is completely soluble [20]. Therefore, temperature and pressure of SFEE were set at 40 °C and 9 MPa, respectively, to ensure that the system would be at the supercritical state. Also, the temperature of 40 °C is mild enough to prevent the organic solvent from reaching the boiling point, in which bubbles could be formed, thus damaging the emulsion droplets and affecting the particle characteristics [21].

2.4. Characterization of the suspensions

2.4.1. Residual ethyl acetate content

The residual ethyl acetate content (REA) of the suspensions was determined using a gas chromatograph with a flame ionization detector (GC-FID, Shimadzu, CG17A, Kyoto/Japan) equipped with a capillary column ZB-Wax plus (Phenomenex, 30 m × 0.18 mm × 0.18 µm). Each sample was filtered (Chormafil Xtra PA-20/25, Macherey-Nagel, Düren/Germany) and 1 µL was injected in the chromatograph. The sample split ratio was 1:100. The carrier gas (Helium, 99.9% purity, White Martins, Campinas/Brazil) flow rate was 2.2 mL/min. The

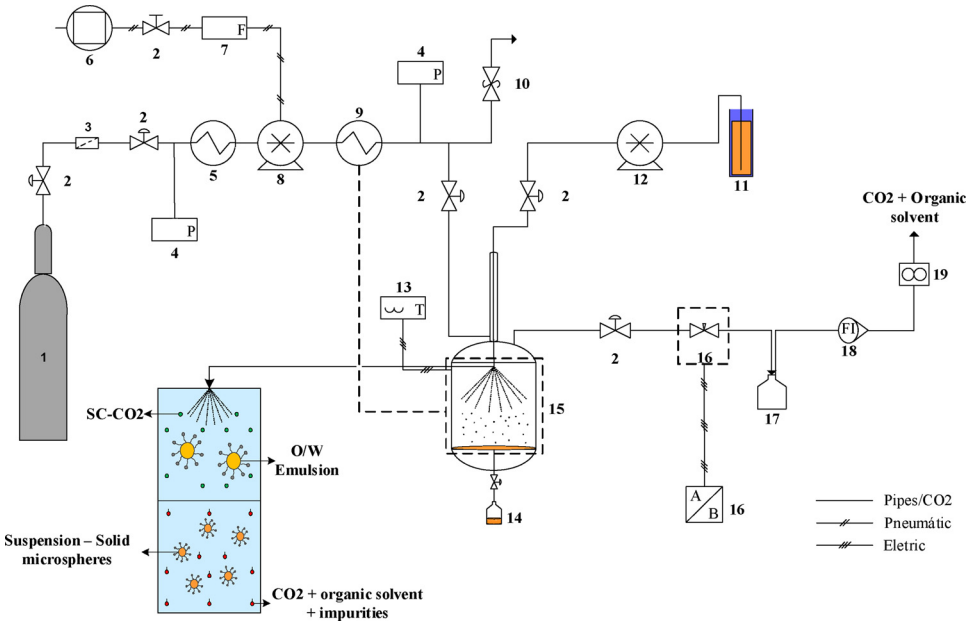

Fig. 1. Schematic diagram of the SFEE unit. (1) CO_2 cylinder; (2) Control valves; (3) CO_2 filter; (4) Pressure indicators (manometers); (5) Cooling bath; (6) Compressor; (7) Compressed air filter; (8) CO_2 pump; (9) Heating bath; (10) Safety valve; (11) Emulsion reservoir (solute/solvent); (12) HPLC pump; (13) Temperature controllers; (14) Suspension; (15) Precipitation column; (16) Micrometric valve with heating system; (17) Glass flask; (18) Flow meter; (19) Gas totalizer.

injector and the detector temperatures were 180 and 220 °C, respectively. The column was heated from 35 °C to 200 °C at 7 °C/min, each one with a hold time of 5 min (35 °C) and 2 min (200 °C), respectively. The retention time of ethyl acetate peak was 2.07 min, and quantification was performed using an external standard calibration curve (R^2 = 0.9999).

2.4.2. Optical microscopy

The suspensions were analyzed in an optical microscope (Carl Zeiss, model Axio Scope A1, Göttingen, Germany), using 100× magnification lens, operating under oil immersion. Aliquots of the suspensions were placed on glass slides and covered with coverslips to be imaged.

2.4.3. Particle diameter

The mean diameters of the suspended particles were determined after 24 h by light scattering (PCS) using a Zeta Potential Analyzer (Brookhaven Instruments Corporation, USA), which is a gauge of particle size by spreading of light, with a 15 mW power solid-state laser and wavelength of 675 nm. The diameters were measured in triplicate.

2.4.4. β-caryophyllene recovery and oleoresin loss

The determination of β-caryophyllene in the suspension was performed by gas chromatography (Agilent Technologies model 6890N, Santa Clara, USA) coupled to a selective mass detector (model MSD 5975, Santa Clara, USA). The compounds were separated in a capillary column HP-5 MS (30 m × 0.25 mm × 0.25 µm) operating at 120 °C, 2 °C/min, 160 °C, 10 °C/min, 300 °C (3 min). Injector split-splitless was used. Helium was the carrier gas with flow rate of 1.0 mL/min. The injector and detector temperatures were 220 and 290 °C, respectively. 1 µL of the suspension was injected into the chromatograph and the quantification of β-caryophyllene (Tr = 23.82 min) was performed using an external standard calibration curve. The identification was based on the retention time of the standard used and the comparison of its mass spectra with those found in the NIST (National Institute of Standards and Technology) electronic database.

The β-caryophyllene recovery was defined as the ratio between the initial mass of β-caryophyllene in the emulsion before SFEE ($M_{initial}$) and the mass of β-caryophyllene in the suspension after SFEE (M_{Final}), as shown in Eq. (1).

$$R_{\beta C} = \frac{M_{Initial}}{M_{Final}} x\ 100 \quad (1)$$

The oleoresin loss was calculated as the ratio between the mass of oleoresin injected in the SFEE system and the residual mass of oleoresin in the collecting flask at the end of the process.

2.5. Characterization of the dried suspensions

After the SFEE, the oleoresin particles that were produced remained suspended in the aqueous phase. The best SFEE condition selected for drying was the one that resulted in the lowest REA in the suspension. Water was removed from the suspension by two drying techniques (*freeze-drying* and *spray-drying*), following the conditions previously established by Pasquel-Reátegui et al. [19]. The dried particles were stored at –18 °C in amber glass vials to be protected from light and oxygen, before characterization by their moisture content, water activity, particle size distribution, x-ray diffraction and morphology by FESEM and CLSM.

2.5.1. Moisture content and water activity

The moisture content of the particles was gravimetrically determined according to the AOAC method 925.10 [22]. The particle samples were placed on previously weighed glass plates and oven dried under forced air circulation (model NT 395-1, Tecnal, São Paulo) at 60 °C for 4 h. Water activity (a_w) was measured at 25 °C in a water activity meter equipment (AquaLab Series 3TE, Decagon, Pullman, USA).

2.5.2. Particle size and distribution

The particle size distributions and their mean diameter were determined by laser diffraction on a Mastersizer 2000 equipment (Malvern Instruments Ltd., Malvern, United Kingdom). The mean particle diameter was based on the mean diameter of a sphere of the same volume, named diameter of De Brouckere ($D_{[4,3]}$), calculated with Eq. (2). The samples were analysed in quintuplicate by the wet method, using ethanol (99.5%).

$$D_{[4,3]} = \frac{\sum n_i d_i^4}{\sum n_i d_i^3} \quad (2)$$

Where d_i is the particle diameter and n_i is the number of particles.

2.5.3. X-ray diffraction

The X-ray diffraction patterns of the particles and polymers were

obtained in a diffractometer (Shimadzu XRD-7000, Tokyo, Japan). The analyses were carried out with radiation source from Cu-Kα (λ = 1.5406 Å), operating at 40 kV/30 mA, and the angle (2 θ) was scanned from 5 to 50° at a 2°/min rate.

2.5.4. Field emission scanning electron microscopy

The morphology of the particles was analyzed in a scanning electron microscope equipped with a field emission gun (FESEM – FEI Quanta 650, USA). Before analysis, the samples were coated with iridium (about. 30 min) in a SCD 050 sputter coater (Oerlikon-Balzers, Balzers, Liechtenstein). Analyses of the sample surfaces were carried out under vacuum, using a 5 kV acceleration voltage.

2.5.5. Confocal laser scanning microscopy

The confocal laser scanning microscopy (CLSM) analyses were performed on the copaiba oleoresin particles without any previous preparation. The particles were analyzed in a Zeiss LSM 780-NLO confocal on an Axio Observer Z.1 microscope (Carl Zeiss AG, Germany), equipped with a 40× objective. The images were obtained at a wavelength of 488 nm, as described by Pasquel-Reátegui et al. [19].

2.6. Statistical analyses

All results are presented as a mean ± standard deviation. To evaluate the statistical differences between the experiments, the Tukey test was performed at a significance level of 5% ($p < 0.05$). Statistical analyses were executed using Minitab statistical software (version 16.2.1, 2016, Minitab Inc.). The results of XRD were analyzed descriptively.

3. Results and discussion

3.1. Droplet size variation

Fig. 2 presents: a) the dispersion (non-emulsified) with a mean droplet diameter of 716 ± 3 nm, and b) the emulsified dispersion, which achieved a 71-fold reduction in the droplet diameter in 10 min. It is worth mentioning that the droplet diameter achieved 262 ± 2 nm after 24 h, and previous works showed that this emulsion has high kinetic stability after 24 h [19]. Based on these results, the emulsion was injected in the SFEE unit before 30 min, since its droplet diameter at this time is below 100 nm. The required time for the stabilization of the SFEE conditions was also considered for this choice.

3.2. SFEE process

The SFEE process consisted in the polymer precipitation since the organic solvent (ethyl acetate) was extracted from the emulsion with supercritical CO_2. Initially, the extraction time was fixed in 30 min. During the SFEE process, some oleoresin was collected in the glass

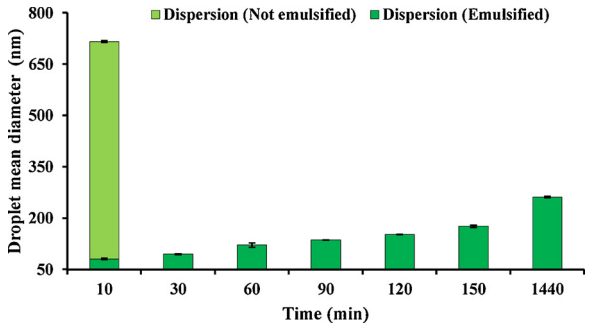

Fig. 2. Influence of time on the mean droplet diameter of the emulsion of copaiba oleoresin produced with ultrasonic power of 480 W and sonication time of 6 min.

flasks, indicating some solubility in supercritical CO_2 under these process conditions. The lowest oleoresin loss was achieved with the highest emulsion flow rate (1.0 mL/min) for all CO_2 flow rates, as shown in Table 1. Similar behavior was found in SFEE for the encapsulation of capsaicinoids from red pepper [15]. The loss of oleoresin by co-extraction is related to the solubility of the oleoresin of copaiba in ethyl acetate and subsequent affinity with the SC-CO_2, causing the ethyl acetate to act as co-solvent in CO_2, thus removing compounds of copaiba oleoresin. Moreover, possible instability of the emulsion during SFEE can lead to the release of oleoresin to the aqueous phase and its further dissolution in supercritical CO_2.

Table 1 shows that the highest reduction in the residual ethyl acetate content was achieved with an emulsion flow rate of 0.5 mL/min, independently of Q_{CO2}. The increase in Q_{CO2} and the reduction of Q_{em} enhanced the removal of ethyl acetate up to 97.1%, achieving REA of 2325 ± 225 ppm in the suspension. The velocity of CO_2 increases with its flow rate, intensifying turbulence and mass transfer inside the high-pressure vessel during the injection of the emulsion, thus resulting in a decrease of ethyl acetate concentration in the suspension. From the results exposed in Table 1 and considering the lowest CO_2 consumption and the lowest REA in the suspension, three experimental conditions (E-1, E-2 and E-5) were selected for additional experiments to evaluate the effect of extraction time. The extraction time may affect the removal rate of ethyl acetate and, therefore, the technical and economic viability of the process. The results of these experiments are presented in Table 2.

The highest reduction of solvent (98.2%) was observed at 60 min of extraction for Q_{em} = 0.5 mL/min and Q_{CO2} = 12.48 g/min, as shown in Table 2. Moreover, REA in the suspension decreases as extraction time increases, but no statistical difference was found between REA at 45 and 60 min for Q_{em} = 0.5 mL/min and both tested SC-CO_2 flow rates (12.48 and 24.42 g/min). High CO_2 flow rates reduce the contact time between supercritical CO_2 and emulsion, resulting in an inefficient extraction of the solvent. Furthermore, the best RAE condition (E-1D) resulted in a suspension with an ethyl acetate content (1484.5 ± 16.0 ppm) legally permitted by the pharmaceutic industry, which must be below 5000 ppm for ethyl acetate [23].

The removal of ethyl acetate in rotary evaporation at 45 °C achieved REA of 7865.0 ± 129.3 ppm in the suspension (Table 2), thus higher than in SFEE. The difference in these methods is the contact area between the suspension and the extraction solvent, which is larger in SFEE, enhancing the elimination rate of ethyl acetate.

It is noted in Tables 1 and 2 that the particle size of the suspensions had small variation (approximately ± 20 nm), using the coaxial nozzle of 177.8 μm at all experimental conditions. Therefore, either SC-CO2 or emulsion flow rates affect the particle size [13,15]. Similar behavior were observed by Della Porta and Reverchon [12] in the production of PLGA/Piroxicam microspheres and by Mezzomo et al. [24] in the encapsulation of emulsions from pink shrimp wastes. The particles produced by SFEE presented monodisperse distribution, which is important for the controlled delivery of the target compounds. The same trend was found in the production of chitosan-based nanosuspensions [25] and encapsulation carotenoids [7]. However, comparing the droplet diameters of the emulsion before and after SFEE, an increase of 2.6 times was observed, although the droplet diameter is still in the nanometre range. Similar behavior was observed by de Paz et al. [26], studying the solubility of β-carotene in poly-(ε-caprolactone) particles produced in colloidal state by SFEE, and by Aguiar et al. [15], who encapsulated red pepper oleoresin by SFEE.

The influence of the coaxial nozzle diameter was also investigated at the condition of experiment E-1D, which achieved the lowest REA. The results show that, as the nozzle diameter decreases, higher is the reduction in REA, achieving 99.2% (662.9 ± 49.5 ppm of ethyl acetate in the suspension), as shown in Table 2. The emulsions injected into the SFEE system with the smallest coaxial nozzle had an increase in droplet size after 24 h as compared to the droplet size of the injected emulsion,

Table 1
Influence of CO_2 and emulsion flow rates in the SFEE at 40 °C and 90 MPa of copaiba oleoresin.

Experiment	SFEE – Coaxial nozzle (177.8 μm)								
	Q_{CO2} (g/min)	S (kg)[a]	Q_{em} (mL/min)	S/F (kg/kg)[b]	REA (ppm)(*)	SR (%)	$D_{[4.3]}$ (nm)	Oleoresin loss (%)	β-caryophyllene recovery (%)(*)
E-1	12.48	0.75	0.5	50	4117 ± 161^{C}	94.1	244.20 ± 3.42	10.06	7.3 ± 0.2^{E}
E-2	12.48	0.75	1.0	25	13619 ± 490^{A}	83.1	240.72 ± 2.43	1.83	12.9 ± 0.2^{A}
E-3	18.60	1.12	0.5	75	3264.3 ± 30.8^{C}	95.9	239.27 ± 2.33	1.39	8.3 ± 0.3^{D}
E-4	18.60	1.12	1.0	37	10554 ± 609^{B}	86.9	281.98 ± 3.99	0.22	10.8 ± 0.1^{B}
E-5	24.42	1.46	0.5	97	2325 ± 225^{C}	97.1	231.35 ± 1.35	6.28	6.8 ± 0.1^{E}
E-6	24.42	1.46	1.0	48	11801 ± 904^{AB}	85.8	249.87 ± 2.63	0.33	9.8 ± 0.2^{C}

Results are expressed as mean ± standard deviation of the analysis. Q_{CO2} = carbon dioxide flow rate; S = mass of injected CO_2; Q_{em} = emulsion flow rate; F = mass of injected emulsion; REA = residual ethyl acetate; SR = solvent reduction; $D_{[4.3]}$ = suspended particles diameter. (*) Equal letters in the same column indicate no significant difference at the level of 5% according to Tukey test.
[a] Considering the injection time of the emulsion (30 min) and drying time (30 min).
[b] Considering the density of the emulsion equal to 995 kg/m^3.

as shown in Fig. 3. According to Li et al. [21], the distance between droplets increases with their size, thus avoiding coalescence. Even so, the droplet size must remain small, since big droplets are less stable in microspheres and risk to leak the target compounds. No flocculation or coalescence was noticed after 24 h, as can be observed in Fig. 3(b). So, the droplets may have expanded due to the *Ostwald ripening* phenomenon – for instance, smaller droplets not covered with starch may have been coalesced into larger droplets because of pressure gradients. Smaller droplets can appear because the emulsion droplet diameter is lower than the coaxial nozzle. The particles are reduced under pressure to flow through the nozzle and have their surface areas increased. Thus, larger Hi-Cap 100® amount, which may not be available, is needed to cover their surface. This behavior can explain the lower REA in the suspension (662.9 ± 49.5 ppm), since larger surface area and less starch core enhance the contact between supercritical CO_2 and ethyl acetate, intensifying its removal.

The β-caryophyllene recovery in the suspensions after SFEE is higher for Q_{em} = 1.0 mL/min for all CO_2 flow rates. Moreover, the highest oleoresin losses coincide with the lowest β-caryophyllene recoveries in the suspensions, as presented in Table 1. Regarding REA, the increase in extraction time intensified the loss of β-caryophyllene, as shown in Table 2. This profile can probably be explained by the dissolution of β-caryophyllene in supercritical CO_2, which might have been enhanced when low content of ethyl acetate was available. Although the β-caryophyllene recovery was low, probably some diterpenic acids, such as copalic acid, must have been encapsulated due to the difference between the solubilities of those compounds in SC-CO_2. Summarizing, the SFEE process with Q_{em} = 0.5 mL/min, Q_{CO2} = 12.48 g/min and 30 min of solvent extraction achieved REA within the limit required by FDA and the highest recovery of β-caryophyllene, being recommended for further investigations.

3.3. Characterization of the suspended particles after drying

3.3.1. Moisture content and water activity

The spray-dried particles presented higher moisture and water activity than those obtained by freeze-drying, as can be noted in Table 3. The high temperature in spray-drying (170 °C) may induce the formation of a barrier on the particle surface, thus hampering the water diffusion and reducing its evaporation rate [27]. Damodaran et al. [28] report that particles with low moisture and water activity are stable in terms of their physical properties, besides presenting slow deterioration reactions and microbial growth, thus increasing their shelf-life. According to Quek et al. [29], a particle can be considered microbiologically stable with a_w below 0.6. Therefore, the particles produced by freeze-drying and those obtained by spray-drying with the 127 μm

Table 2
Influence of solvent extraction time in the SFEE at 40 °C and 90 MPa of copaiba oleoresin.

Experiment	t (min)	Q_{CO2} (g/min)	Q_{em} (mL/min)	REA (ppm)(*)	S (kg)[a]	S/F (kg)[b]	SR (%)	$D_{[4.3]}$ (nm)	β-caryophyllene recovery (%)(*)
E-1A	15	12.48	0.5	5567.6 ± 66.3^{CD}	0.187	12.4	93.1	242.60 ± 4.38	9.1 ± 0.2^{C}
E-1B	30			4117 ± 161^{D}	0.374	25.0	94.1	244.20 ± 3.42	7.3 ± 0.2^{D}
E-1C	45			1757.7 ± 47.8^{EF}	0.561	37.4	97.8	251.53 ± 4.61	6.9 ± 0.3^{DE}
E-1D	60			1485.5 ± 16.0^{EF}	0.749	50.0	98.2	262.27 ± 2.01	5.7 ± 0.6^{EF}
E-2A	15	12.48	1.0	14091 ± 948^{A}	0.187	6.20	82.5	241.23 ± 2.58	13.8 ± 1.1^{A}
E-2B	30			13619 ± 490^{A}	0.374	12.5	83.1	240.72 ± 2.43	12.9 ± 0.2^{A}
E-2C	45			7525 ± 606^{B}	0.561	18.7	90.6	261.57 ± 0.42	10.8 ± 0.2^{B}
E-2D	60			7009 ± 542^{BC}	0.749	25.0	91.3	294.70 ± 4.93	7.6 ± 0.1^{D}
E-5A	15	24.42	0.5	4425 ± 381^{D}	0.366	24.4	94.5	245.40 ± 0.52	7.2 ± 0.5^{D}
E-5B	30			2325 ± 225^{E}	0.732	48.8	97.1	231.35 ± 1.35	6.8 ± 0.1^{DE}
E-5C	45			2129.1 ± 160.1^{EF}	1.100	73.3	97.3	266.30 ± 1.70	5.2 ± 0.2^{FG}
E-5D	60			2006.3 ± 100.5^{EF}	1.465	97.7	97.5	282.37 ± 3.01	4.2 ± 0.1^{G}
SFEE – Coaxial nozzle (127 μm)									
E-1D	60	12.48	0.5	662.9 ± 49.5^{G}	0.749	50.0	99.2	532.87 ± 6.17	2.0 ± 0.1^{H}
Evaporation of ethyl acetate - rotary evaporator									
E-6	60	–	–	7865.0 ± 129.3^{B}	–	–	90.2	5.1 ± 0.1^{FG}	

Results are expressed as mean ± standard deviation. t = solvent extraction time; Q_{CO2} = carbon dioxide flow rate; Q_{em} = emulsion flow rate; REA = residual ethyl acetate; S = mass of injected CO_2; F = mass of injected emulsion; SR = solvent reduction; $D_{[4.3]}$ = suspended particles diameter. (*) Equal letters equal in the same column indicate no significant difference at the level of 5% according to Tukey test.
[a] Considering the injection time of the emulsion (30 min) and drying time.
[b] Considering the density of the emulsion equal to 995 kg/m^3.

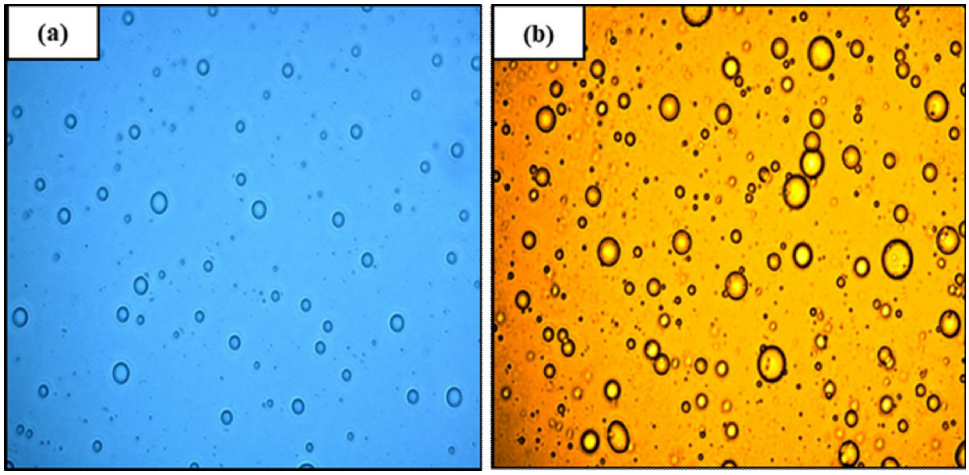

Fig. 3. Image of optical microscopy: (a) emulsion before SFEE, and (b) suspension after 24 h, obtained with coaxial nozzle of smaller diameter (127 μm) after removal of ethyl acetate.

Table 3
Characterization of the suspended particles after freeze-drying (FD) and spray-drying (SD).

Particle	Moisture (%)	a_w	Particle diameter (μm)
SFEE – Coaxial nozzle (177.8 μm) - FD	0.88 ± 0.05^{C}	0.15 ± 0.01^{BC}	238.72 ± 0.79^{B}
SFEE – Coaxial nozzle (127 μm) - FD	0.73 ± 0.06^{C}	0.09 ± 0.01^{C}	277.75 ± 5.81^{A}
SFEE – Coaxial nozzle (177.8 μm) - SD	2.36 ± 0.12^{A}	0.62 ± 0.04^{A}	10.52 ± 0.64^{C}
SFEE – Coaxial nozzle (127 μm) - SD	1.80 ± 0.08^{B}	0.17 ± 0.01^{B}	14.68 ± 1.44^{C}

Results are presented as mean ± standard deviation. a_w = water activity. Equal letters in the same column indicate no significant difference at the level of 5% according to Tukey test.

nozzle are resistant to microorganisms. Pasquel-Reátegui et al. [19] observed that the freeze-dried particles present higher oxidative stability than the non-encapsulated copaiba oleoresin. Moreover, the particle moistures were quite low for all methods, which assures them small decomposition rates, which are typical in moistures below 5% [30].

3.3.2. Particle size distribution

Spray-drying produced particles around 10–15 μm with no statistical effect of the nozzle diameter in SFEE. The achieved particle size was expected for this method, as well as those of freeze-drying, which can reach 300 μm [31,32]. The large particles produced in freeze-drying are a consequence of the low temperature and energy available to break the frozen droplets. Drying by spray-drying and freeze-drying presented bimodal and monomodal size distribution, respectively, as shown in Fig. 4. Similar result was observed by Pasquel-Reátegui et al. [19] in copaiba oleoresin particles encapsulated in modified starch.

3.3.3. X-ray diffraction

Fig. 5 presents the diffractograms of pure Hi-Cap 100® and particles obtained by spray-drying and freeze-drying. The dried particles and the starch behave as amorphous materials, indicating that neither SFEE nor the drying methods affected the starch's structural properties. Amorphous materials exhibit amorphous halos in XRD and are usually more soluble and hygroscopic than the crystalline ones, since the molecules in the amorphous state are disordered [33,34]. Powders with amorphous characteristics hydrate rapidly due to the low energy levels of the bonds between molecules when compared to the crystalline state [35].

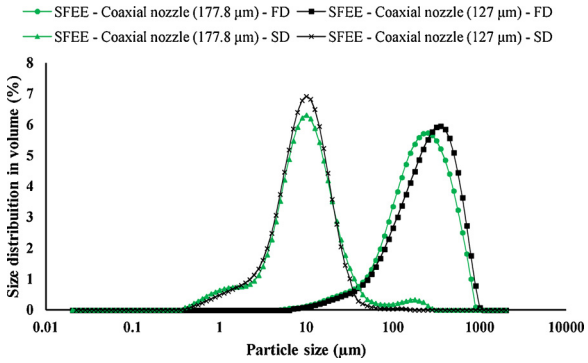

Fig. 4. Particle size distribution obtained after freeze-drying (FD) and spray-drying (SD) of the suspensions obtained by SFEE.

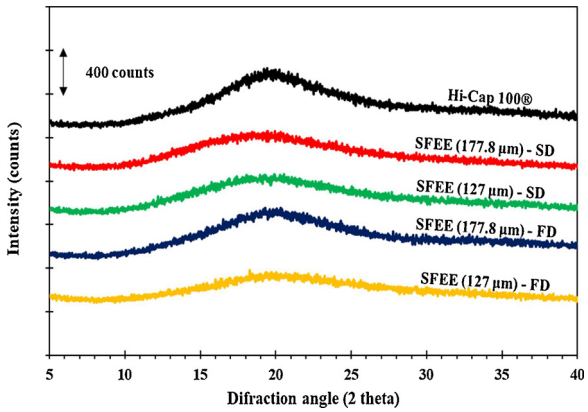

Fig. 5. X-ray diffraction of Hi-Cap 100® and suspensions after freeze-drying (FD) and spray-drying (SD).

Similar behavior was observed in copaiba oleoresin particles encapsulated in modified starch, using Hi-Cap 100® and Snow-Flake® E 6131 as polymer, and dried by freeze-drying and spray-drying [19].

3.3.4. Microstructural analysis of the particles

The freeze-dried particles presented irregular elongated structures, similar to flat sheets (Fig. 6(a) and (b)), as typically found in freeze-dried samples [31,36]. Small pores are also observed on the inner particle walls (Fig. 6(c) and (d)), which may have been formed by the agglomeration of emulsion droplets during freezing and drying [19], which remain attached by the starch layer. Similar microstructures

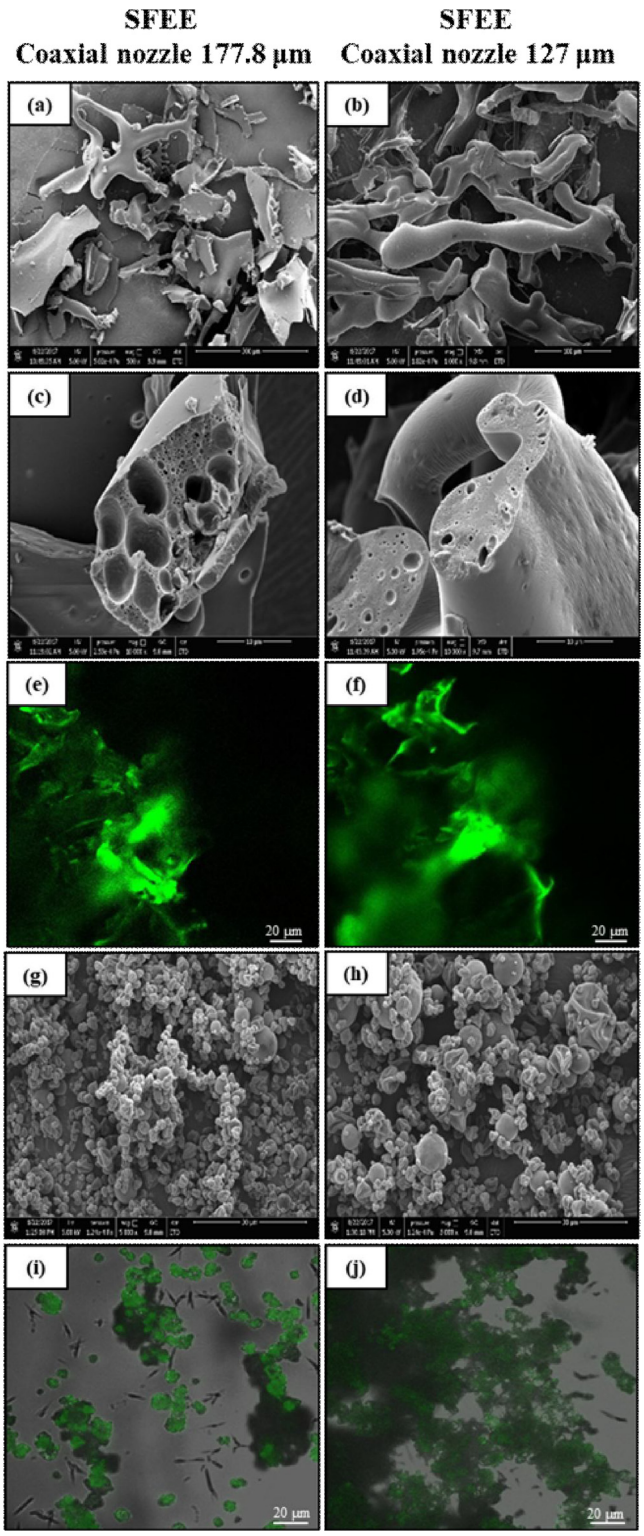

Fig. 6. FESEM and CLSM images of the particles produced after freeze-drying (500X (a), 1000X (b) and 10000X (c) and (d) magnification – CLSM (e) and (f)) and spray-drying (5000X (g) and (h) magnification – CLSM (i) and (j)) of the suspension obtained by SFEE (Q_{CO2} = 12.48 g/min, Q_{em} = 0.5 mL/min and 60 min of solvent extraction time) (For interpretation of the references to colour in this figure legend, the reader is referred to the web version of this article).

were also reported in the freeze-drying of annatto seed oil [37] pepper oleoresin [15], and limonene particles [38].

The spray-dried particles have spherical shapes with different sizes. Their surfaces do not present fissures or cracks, thus providing enhanced protection and retention of the target compounds within their nuclei, as shown in Fig. 6 (g) and (h). Nevertheless, rough surfaces are also observed, possibly originated from water evaporation that leads to the core solidification before the expansion of particles, and thus their shrinkage in drying [7,19,39].

The CLSM images of the particles obtained by freeze-drying (Fig. 6(e) and (f)) and spray-drying (Fig. 6(i) and (j)) reveal the impregnation of the active material (green colour) in the particles, thus confirming the encapsulation of copaiba oleoresin in Hi-Cap 100®. Unlike modified starch, copaiba oleoresin has some fluorescence that allows observing the internal particle structure without damaging the target compounds [40].

4. Conclusions

Supercritical fluid extraction of emulsions (SFEE) was successfully applied to produce copaiba oleoresin particles with residual ethyl acetate content within the legal limits. The SFEE process at flow rates of 0.5 mL/min and 12.48 g/min for emulsion and SC-CO_2, respectively, with 30 min of solvent extraction, provided the highest β-caryophyllene recovery in the particles. This recovery decreased at low ethyl acetate concentration, indicating a negative influence of solvent extraction time due to the solubilization of β-caryophyllene in supercritical CO_2. Although the β-caryophyllene recovery was low, it is possible that diterpenic acids have been encapsulated. The particle size of the suspensions produced in SFEE had small variation from the emulsion droplet diameter, indicating that both dimensions are strongly correlated.

Freeze-drying and spray-drying were applied to dry the suspensions obtained by SFEE and resulted in particles with different morphologies and sizes. The CLSM images confirmed the encapsulation of copaiba oleoresin in the modified starch Hi-Cap 100®. Therefore, SFEE is capable of encapsulating copaiba oleoresin and leaving an acceptable residual ethyl acetate amount in the product. The diameter of the SFEE coaxial nozzle affects the particle size, but additional investigations are needed to elucidate such influence and propose the scale-up of the process, for its economic evaluation. Several applications of copaiba oleoresin particles can be suggested in cosmetic and pharmaceutic industries, where the properties of its components can provide high added-value products. Depending on the application, either suspended or dried particles may be feasible.

Acknowledgments

The authors thank CAPES, by the doctorate scholarship and financial support of the project, also FAPESP (grants 2006/03262-9, 2007/58017-5, 2009/54137-1, 2012/22119-7, 2015/11932-7 and 2016/13602-7) for financial support, and the National Institute of Science and Technology on Photonics Applied to Cell Biology (INFABIC) at the University of Campinas for the access to equipments and the provided assistance.

References

[1] L.A.F. Paiva, L.A. Gurgel, R.M. Silva, A.R. Tomé, N.V. Gramosa, E.R. Silveira, F.A. Santos, V.S.N. Rao, Anti-inflammatory effect of kaurenoic acid, a diterpene from *Copaifera langsdorffii* on acetic acid-induced colitis in rats, Vasc. Pharmacol. 39 (2002) 303–307.
[2] S.R.M. Lima, V.F. Veiga Jr, H.B. Christo, A.C. Pinto, P.D. Fernandes, In vivo and in vitro studies on the anticancer activity of *Copaifera multijuga Hayne* and its fractions, Phytother. Res. 17 (2003) 1048–1053.
[3] L.A.F. Paiva, L.A. Gurgel, A.R. Campos, E.R. Silveira, V.S.N. Rao, Attenuation of ischemia/reperfusion-induced intestinal injury by oleo-resin from *Copaifera langsdorffii* in rats, Life Sci. 75 (2004) 1979–1987.
[4] J.P.B. Sousa, A.P.S. Brancalion, A.B. Souza, I.C.C. Turatti, S.R. Ambrósio, N.A.J.C. Furtado, N.P. Lopes, J.K. Bastos, Validation of a gas chromatographic method to quantify sesquiterpenes in copaiba oils, J. Pharm. Biomed. Anal. 54 (2011) 653–659.
[5] A.C. Pinto, W.F. Braga, C.M. Rezende, F.M.S. Garrido, V.F. Veiga Jr., L. Bergter,

M.L. Patitucci, O.A.C. Antunes, Separation of acid diterpenes of copaifera cearensis *Huber* ex *Ducke* by flash chromatography using potassium hydroxide impregnated silica gel, J. Braz. Chem. Soc. 11 (2000) 355–360.
[6] V.F. Veiga Junior, A.C. Pinto, The Copaifera L. Genus, Quím. Nova 25 (2002) 273–286.
[7] D.T. Santos, Á. Martín, M.A.A. Meireles, M.J. Cocero, Production of stabilized submicrometric particles of carotenoids using supercritical fluid extraction of emulsions, J. Supercrit. Fluids 61 (2012) 167–174.
[8] C. Wischke, S.P. Schwendeman, Principles of encapsulating hydrophobic drugs in PLA/PLGA microparticles, Int. J. Pharm. 364 (2008) 298–327.
[9] D. Horn, J. Rieger, Organic nanoparticles in the aqueous phase—theory, experiment, and use, Angew. Chem. Int. Ed. 40 (2001) 4330–4361.
[10] J. Jung, M. Perrut, Particle design using supercritical fluids: literature and patent survey, J. Supercrit. Fluids 20 (2001) 179–219.
[11] G. Della Porta, R. Campardelli, E. Reverchon, Monodisperse biopolymer nanoparticles by continuous supercritical emulsion extraction, J. Supercrit. Fluids 76 (2013) 67–73.
[12] G. Della Porta, E. Reverchon, Nanostructured microspheres produced by supercritical fluid extraction of emulsions, Biotechnol. Bioeng. 100 (2008) 1020–1033.
[13] P. Chattopadhyay, R. Huff, B.Y. Shekunov, Drug encapsulation using supercritical fluid extraction of emulsions, J. Pharm. Sci. 95 (2006) 667–679.
[14] F. Mattea, Á. Martín, A. Matías-Gago, M.J. Cocero, Supercritical antisolvent precipitation from an emulsion: β-carotene nanoparticle formation, J. Supercrit. Fluids 51 (2009) 238–247.
[15] A.Cd. Aguiar, L.P.S. Silva, C.Ad. Rezende, G.F. Barbero, J. Martínez, Encapsulation of pepper oleoresin by supercritical fluid extraction of emulsions, J. Supercrit. Fluids 112 (2016) 37–43.
[16] J. Kluge, F. Fusaro, N. Casas, M. Mazzotti, G. Muhrer, Production of PLGA micro- and nanocomposites by supercritical fluid extraction of emulsions: I. Encapsulation of lysozyme, J. Supercrit. Fluids 50 (2009) 327–335.
[17] J. Kluge, F. Fusaro, M. Mazzotti, G. Muhrer, Production of PLGA micro- and nanocomposites by supercritical fluid extraction of emulsions: II. Encapsulation of Ketoprofen, J. Supercrit. Fluids 50 (2009) 336–343.
[18] J. Kluge, L. Joss, S. Viereck, M. Mazzotti, Emulsion crystallization of phenanthrene by supercritical fluid extraction of emulsions, Chem. Eng. Sci. 77 (2012) 249–258.
[19] J.L. Pasquel Reátegui, F.M. Barrales, C.A. Rezende, C.L. Queiroga, J. Martínez, Production of Copaiba oleoresin particles from emulsions stabilized with modified starches, Ind. Crops Prod. 108 (2017) 128–139.
[20] M.B. King, A. Mubarak, J.D. Kim, T.R. Bott, The mutual solubilities of water with supercritical and liquid carbon dioxides, J. Supercrit. Fluids 5 (1992) 296–302.
[21] M. Li, O. Rouaud, D. Poncelet, Microencapsulation by solvent evaporation: state of the art for process engineering approaches, Int. J. Pharm. 363 (2008) 26–39.
[22] AOAC, Official Methods of Analysis of the Association of the Official Analytical Chemists, Assoc. Off. Anal. Chem., Arlington, 1997 v. 2.
[23] Guidance for Industry QC3- Tables and List, U.S. Department of Health and Human Services, Food and Drug Administration (FDA), Center for Drug Evaluation and Research (CDER), Center for Biologics Evaluation and Research (CBER), 2017, https://www.fda.gov/downloads/drugs/guidancecomplianceregulatoryinformation/guidances/ucm073395.pdf.
[24] N. Mezzomo, Ed. Paz, M. Maraschin, Á. Martín, M.J. Cocero, S.R.S. Ferreira, Supercritical anti-solvent precipitation of carotenoid fraction from pink shrimp residue: effect of operational conditions on encapsulation efficiency, J. Supercrit. Fluids 66 (2012) 342–349.
[25] Y. Murakami, Y. Shimoyama, Production of nanosuspension functionalized by chitosan using supercritical fluid extraction of emulsion, J. Supercrit. Fluids 128 (2017) 121–127.
[26] E. de Paz, S. Rodríguez, J. Kluge, Á. Martín, M. Mazzotti, M.J. Cocero, Solubility of β-carotene in poly-(ε-caprolactone) particles produced in colloidal state by supercritical fluid extraction of emulsions (SFEE), J. Supercrit. Fluids 84 (2013) 105–112.
[27] E.C. Frascareli, V.M. Silva, R.V. Tonon, M.D. Hubinger, Effect of process conditions on the microencapsulation of coffee oil by spray drying, Food Bioprod. Process. 90 (2012) 413–424.
[28] S. Damodaran, K.L. Parkin, O.R. Fennema, Fennema's Food Chemistry, fourth edition, CRC Press, 2007.
[29] S.Y. Quek, N.K. Chok, P. Swedlund, The physicochemical properties of spray-dried watermelon powders, Chem. Eng. Process. 46 (2007) 386–392.
[30] R.V. Tonon, C. Brabet, M.D. Hubinger, Anthocyanin stability and antioxidant activity of spray-dried açai (*Euterpe oleracea Mart.*) juice produced with different carrier agents, Food Res. Int. 43 (2010) 907–914.
[31] C. Yamashita, M.M.S. Chung, C. dos Santos, C.R.M. Mayer, I.C.F. Moraes, I.G. Branco, Microencapsulation of an anthocyanin-rich blackberry (*Rubus spp.*) by-product extract by freeze-drying, LWT Food Sci. Technol. 84 (2017) 256–262.
[32] Y.B. Che Man, J. Irwandi, W. Abdullah, Effect of Different Types of Maltodextrin and Drying Methods on Physicochemical and Sensory Properties of Encapsulated Durian Flavor, (1999).
[33] L. Wu, J. Zhang, W. Watanabe, Physical and chemical stability of drug nanoparticles, Adv. Drug Deliv. Rev. 63 (2011) 456–469.
[34] L. Yu, Amorphous pharmaceutical solids: preparation, characterization and stabilization, Adv. Drug Deliv. Rev. 48 (2001) 27–42.
[35] R.Vd.B. Fernandes, S.V. Borges, E.K. Silva, Y.F. da Silva, H.J.B. de Souza, E.L. do Carmo, C.R. de Oliveira, M.I. Yoshida, D.A. Botrel, Study of ultrasound-assisted emulsions on microencapsulation of ginger essential oil by spray drying, Ind. Crops Prod. 94 (2016) 413–423.
[36] L. Franceschinis, D.M. Salvatori, N. Sosa, C. Schebor, Physical and functional properties of blackberry freeze- and spray-dried powders, Drying Technol. 32 (2014) 197–207.
[37] E.K. Silva, V.M. Azevedo, R.L. Cunha, M.D. Hubinger, M.A.A. Meireles, Ultrasound-assisted encapsulation of annatto seed oil: whey protein isolate versus modified starch, Food Hydrocoll. 56 (2016) 71–83.
[38] V. Kaushik, Y.H. Roos, Limonene encapsulation in freeze-drying of gum Arabic–sucrose–gelatin systems, LWT - Food Sci. Technol. 40 (2007) 1381–1391.
[39] A. Gharsallaoui, R. Saurel, O. Chambin, A. Voilley, Pea (Pisum sativum, L.) protein isolate stabilized emulsions: a novel system for microencapsulation of lipophilic ingredients by spray drying, Food Bioproc. Techol. 5 (2011) 2211–2221.
[40] B.L. Strand, Y.A. Mørch, T. Espevik, G. Skjåk-Bræk, Visualization of alginate-poly-L-lysine-alginate microcapsules by confocal laser scanning microscopy, Biotechnol. Bioeng. 82 (2003) 386–394.